sustainability

MDPI

Article

A Modeling Study Focused on Improving the Aerodynamic Performance of a Small Horizontal Axis Wind Turbine

Sikandar Khan

Department of Mechanical Engineering, King Fahd University of Petroleum and Minerals, Dhahran 31261, Saudi Arabia; sikandarkhan@kfupm.edu.sa

Abstract: The excessive burning of the fossil fuels has excessively changed the global temperature in the last few decades. The global warming caused due to the burning of the fossil fuels has initiated a need of increasing the use of renewal energy sources. The wind energy is one of the renewable energy sources that can mitigate the excessive global dependency on the fossil fuels. For locations with low-to-medium wind speeds (less than 7 m/s), the main problem is with the starting of the wind turbine. To start a stationary wind turbine, not only is it necessary to overcome the inertia and static friction of the turbine, but the angle of incidence of the wind relative to blade profile also needs to be favorable. Thus, at low wind speeds, the resulting low torque is not enough to start the turbine. It is, therefore, necessary to incorporate a good starting torque in the design requirements of turbines. In this paper, a modeling study is performed using the Pro/E, ADAMS and MATLAB software to improve the starting behavior of a horizontal axis wind turbine for the Cherat location in the northern areas of Pakistan. The yearly average wind speed in the northern areas of Pakistan is less than 5 m/s. The blade element momentum (BEM) theory is used to calculate the optimized wind turbine blade parameters (blade angles and chord lengths) that correspond to the maximum starting torque. Based on the optimized wind turbine blade parameters, Pro/E models were developed and imported to ADAMS software to calculate the torque. As compared to the initial wind turbine model, for the optimized wind turbine model, the starting torque increased from 22.5 N-m to 28 N-m and the coefficient of performance (COP) increased from 0.42 to 0.49 at a tip–speed ratio of 4. The starting torque of the wind turbine should exceed the resistive torques due to bearing friction, generator static, dynamic torque and the inertia of the rotor in order to start the wind turbine. The starting behavior of the horizontal axis wind turbine was successfully improved, and the optimized wind turbine model showed an increased starting torque for low-to-medium wind speed ranges.

Keywords: starting of wind turbine; blade aerodynamic forces; wind turbine coefficient of performance; wind turbine output power; wind turbine output torque

Citation: Khan, S. A Modeling Study Focused on Improving the Aerodynamic Performance of a Small Horizontal Axis Wind Turbine. *Sustainability* **2023**, *15*, 5506. https://doi.org/10.3390/su15065506

Academic Editor: Firoz Alam

Received: 12 January 2023
Revised: 1 March 2023
Accepted: 9 March 2023
Published: 21 March 2023

1. Introduction

The excessive emission of greenhouse gases in the past few decades has caused global warming [1]. In order to mitigate global warming, the level of carbon dioxide in the atmosphere should be reduced. The sequestration of the emitted carbon dioxide in deep sedimentary reservoirs [2] and its conversion to fuels and useful chemical will solve the global environmental problems [3]. It is necessary to reduce the use of fossil fuels on the local and global scales. The use of renewable energy sources such as wind [4], solar [5], geothermal [6], hydro [7] and biomass [8] can alleviate global dependency on fossil fuels. The wind energy is one of the most used renewable source in the last few decades. A wind turbine converts the kinetic energy of the wind into mechanical energy in the first stage. In the second stage, this mechanical energy is converted into electrical energy. The rotation of the wind turbine, due to the aerodynamic forces, creates a torque at the wind turbine shaft. The mechanical energy produced at the shaft is converted into electrical energy by using a generator [9]. Although wind energy has the advantage that it can be utilized

around the clock, its main problem is the sudden variation in the magnitude and direction of the incoming wind with time [10].

In the last two decades, electricity production from wind energy has increased rapidly due to the global concern about global warming [11,12]. In 2021, the electricity generation from the wind energy increased by 17%. This growth in the electricity generation was 55% higher than the growth in 2020. In 2000, the installed capacity of the wind power was 17 GW, which increased to 194 GW in 2010, and in 2021, the installed capacity of the wind power increased to 830 GW. In 2020, China remains at the top in wind power production, with an installed wind power capacity of 288 GW; the USA remains in second place, with a wind power capacity of 122 GW; Germany stands in third place, with a wind power capacity of 62 GW; India remains in fourth place, with a wind power capacity of 39 GW and Spain remains in fifth place, with a wind power capacity of 27 GW [13].

There are various types of wind turbines. All the wind turbines consist of some basic design elements, such as the rotor, gearbox, generator, transformer, control system, yaw drive, tower and the basement. Based on the direction of the axis of the wind turbine, the wind turbines may be classified as horizontal axis and vertical axis wind turbines [14]. Based on the wind speed, the wind turbines can be classified as low-speed wind turbines (Reynolds number (Re) < 10^3), medium-speed wind turbines (10^3 < Re < 10^5) and high-speed wind turbines with Re > 10^5 [15]. Based on the position of the wind turbine with respect to the wind flow direction, the wind turbine can be classified as an upwind-positioned wind turbine or downwind-positioned wind turbine [16]. The wind turbine may be of lift or drag type based on the type of aerodynamics. Based on the number of blades, the wind turbine may be a single-bladed or multi-bladed wind turbine. On the basis of the location where the wind turbine is installed, the wind turbine may be an onshore or offshore wind turbine [17].

The most used type of the wind turbine is the horizontal axis wind turbine (HAWT) due to its high capacity factor [18]. For the regions with high magnitudes of wind speeds, large wind turbine models can be utilized but in the regions with low-to-medium wind speeds, the large wind turbine will encounter a problem during the starting phase. The low wind speed is normally not enough to overcome the starting inertia of a large wind turbine model. Normally, small wind turbine models are utilized in regions with low-to-medium wind speeds [19]. According to the International Electrochemical Commission (IEC), a small wind turbine is one that has a rotor swept area of less than 200 m^2, and which corresponds to a rated power of 50 kW [20]. In the regions with low-to-medium wind speeds, normally, small wind turbine models are installed [21]. During the starting phase of the wind turbine in low wind speed regions, the lift-to-drag ratio of the wind turbine blade is low and the angle of attack is normally high, which restricts the starting of the wind turbine [22]. Chu et al. [23] proposed a folding-blade design for the horizontal axis wind turbine in order improve the starting behavior of the wind turbine. Samuel et al. [24] presented a modified vented NACA0012 aerofoil in an effort to increase the torque produced by a wind turbine at a low tip–speed ratio (TSR). The literature review shows that a great amount of research is needed to come up with optimized wind turbine blade profiles that can achieve high starting torques and can start the wind turbines even at low wind speeds. Salih et al. [25] performed an experimental and theoretical investigation of a micro wind turbine for improving the starting behavior of the wind turbine in low wind speed regions. Wright and Wood [26] investigated the starting performance of a three-bladed, 2 m diameter horizontal axis wind turbine in field tests, and compared it with a quasi-steady blade element analysis. Ebert and Wood [27] used a quasi-steady analysis for improving the starting behavior of the wind turbine that is operated at high angles of attack and a low Reynolds number.

Supakit et al. [28] proposed an analogy between the aerofoil in the Darrieus motion and flapping-wing flow mechanisms. Based on this analogy, the unsteadiness could be exploited for generating additional thrust, and the rotor geometry is the main source of this unsteady thrust. For self-starting, it is necessary that the rotors exploit this unsteadiness. It was

concluded that self-starting rotors may be designed through an appropriate selection of blade aspect and chord-to-diameter ratios. Sun et al. [29] investigated the effect of offsetting pitching angles and blade numbers on the power extraction performance and self-starting characteristics of the vertical axis wind turbine (VAWT). Due to the fact that the vortex separation could be suppressed or delayed due to offsetting the pitching angle and blade number, the starting performance of the wind turbine will be improved. Mohamed et al. [30] investigated the aerodynamics of Darrieus turbines during start-up using a two-dimensional CFD approach. The ANSYS-FLUENT solver was utilized to perform the fluid–structure interaction simulation. The results showed that the blade local absolute velocity (V∞, L) is dependent on the instantaneous tip–speed ratio during the starting revolutions of the rotor.

In this paper, a modeling study is performed for improving the starting behavior of a small horizontal axis wind turbine. An optimization study is performed in the current study in order to have a wind turbine design that will be able to start and operate at the specified low wind speeds. During the optimization process, a novel methodology is utilized in which the effects of changing the wind turbine blade parameters (chord lengths and blade angles) near the hub of the wind turbine on the starting torque of the wind turbine is evaluated. In this novel methodology, the optimized blade parameters were calculated near the hub of wind turbine (in the nine stations near to hub of the wind turbine blades). The model developed in Pro/E, based on the optimized blade parameters, was simulated in ADAMS to find the output torque. ADAMS considers the mass and inertia of the wind turbine, and also the resistive torques due to bearing friction, generator static and dynamic torque, which provide more accurate estimation of the starting torque. The northern areas of Pakistan, having an average wind speed of less than 5 m/s, are considered in this study. The blade element momentum (BEM) theory is used to calculate the optimized wind turbine blade parameters (blade angles and chord lengths) that correspond to the maximum starting torque. Based on the optimized wind turbine blade parameters, Pro/E models were developed and imported to ADAMS software to calculate the torque. The coefficient of performance (COP) and the output torque were calculated for various designs in order to obtain an optimized wind turbine model for the location considered in this study. The starting behavior of the horizontal axis wind turbine was successfully improved, and the optimized wind turbine model showed an increased starting torque for low-to-medium wind speed ranges. The optimized wind turbine design was able to start and operate at the average wind speeds of less than 5 m/s for the northern areas of Pakistan.

2. Governing Equations

The blade element momentum (BEM) theory can be used for the analysis of an existing wind turbine and for designing a blade profile for a specific wind speed. The BEM theory is explained below [31].

Using the BEM theory, the axial force and torque can be calculated by considering momentum balance at various sections.

As shown in Figure 1, a stream tube is shown around the wind turbine. Four sections are shown: Section 1, some way upstream the wind turbine; Section 2, just before the wind turbine blades; Section 3, just after the wind turbine blades; and Section 4, some way downstream the wind turbine. Between Sections 2 and 3, energy is extracted from the wind so there is a change in pressure. If we assume the pressure at Section 1 is equal to the pressure at Section 4, the velocity at Section 2 is equal to the velocity at Section 3, and the flow between Sections 1 and 2 and Sections 3 and 4 is frictionless, then by Bernoulli's equation:

$$P_2 - P_3 = \frac{1}{2}\rho\left({V_1}^2 - {V_4}^2\right) \quad (1)$$

where P_2 = pressure at Point 2, P_3 = pressure at Point 3, V_1 = upstream wind velocity, V_4 = downstream wind velocity, and ρ is the density of air.

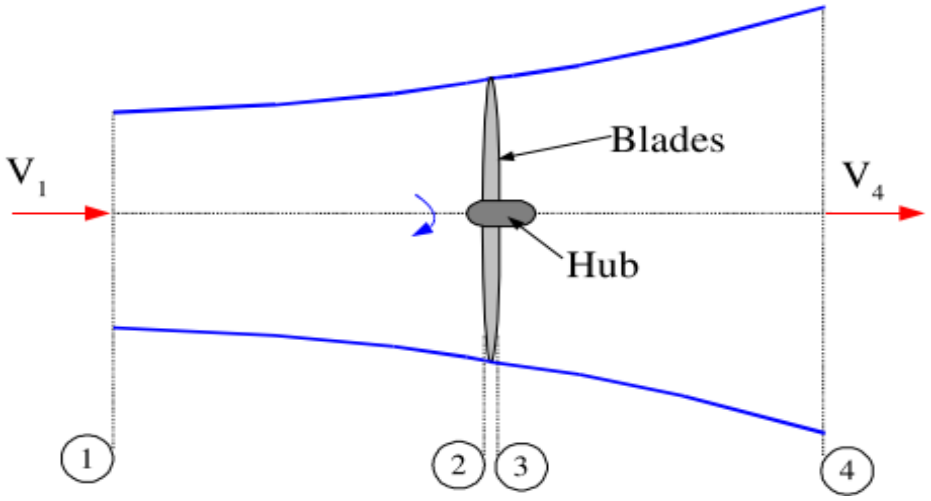

Figure 1. Stream tube for axial forces on wind turbine [31].

The axial force (dF_x) can be found by multiplying pressure with area (dA) as follows

$$dF_x = (P_2 - P_3)dA \quad (2)$$

Putting the value of pressure difference from Equation (1) into Equation (2) will give

$$dF_x = \frac{1}{2}\rho\left({V_1}^2 - {V_4}^2\right)dA \quad (3)$$

The axial induction factor accounts for the loss in absolute velocity (V) when the incoming wind comes in contact with wind turbine blades. The axial induction factor (a) is given as

$$a = \frac{V_1 - V_2}{V_1} \quad (4)$$

After some calculation, the following two equations are obtained

$$V_2 = V_1(1 - a) \quad (5)$$

$$V_4 = V_1(1 - 2a) \quad (6)$$

Putting the values of V_2 and V_4 in Equation (3) will give the following equation

$$dF_x = \frac{1}{2}\rho{V_1}^2[4a(1 - a)2\pi r dr] \quad (7)$$

In order to derive an expression for the torque, consider the rotating annular stream tube as shown in Figure 2.

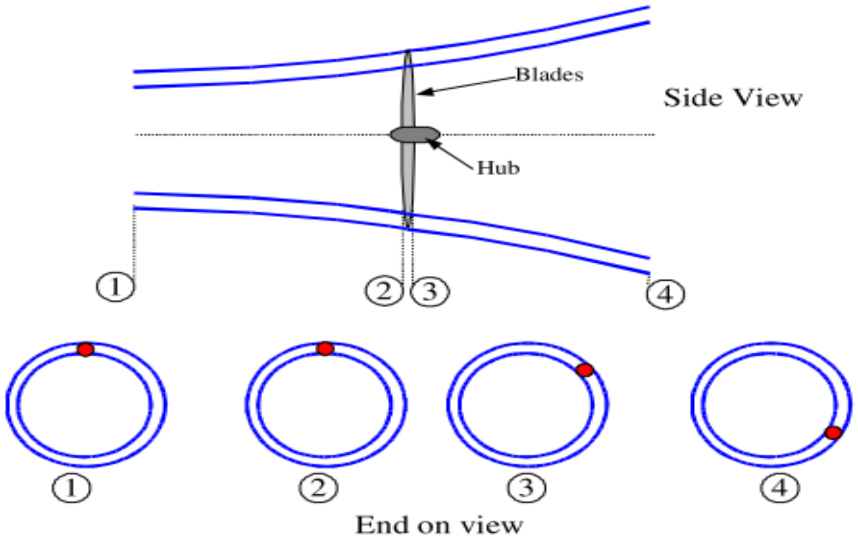

Figure 2. Stream tube for the tangential forces on wind turbine [31].

Four sections are shown in Figure 2: Section 1, some way upstream the wind turbine; Section 2, just before the wind turbine blades; Section 3, just after the wind turbine blades; and Section 4, some way downstream the wind turbine. In order to derive an equation for the torque, it is necessary to consider the conservation of angular momentum. Consider Figure 3, which shows the angular velocity of blade wake (ω) and the angular velocity of blade (Ω).

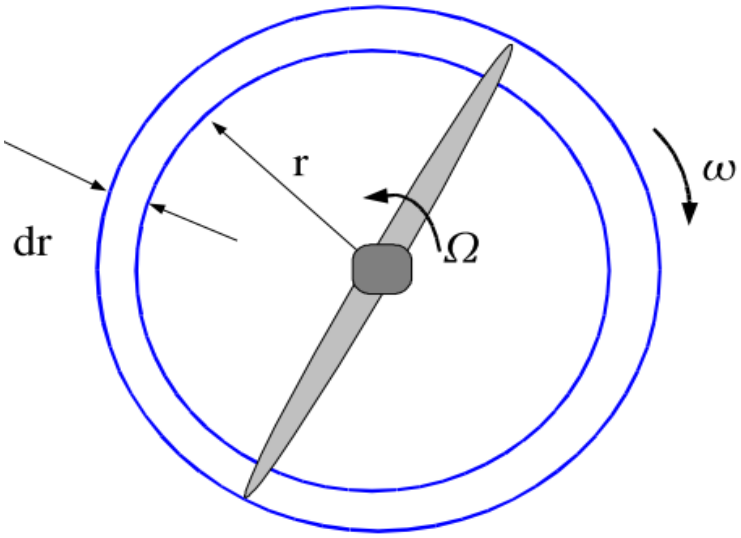

Figure 3. Angular velocities of blade and blade wake [31].

From the elementary knowledge of physics, it is know that

Moment of inertia of annulus, $I = mr^2$, angular moment, $L = I\omega$, and torque $T = dL/dt$, so

$$T = \frac{dI\omega}{dt} = \frac{d(mr^2\omega)}{dt} = \frac{dm}{dt}r^2\omega \quad (8)$$

The torque for the small element can also be written as

$$dT = d\dot{m}r^2\omega \quad (9)$$

From the continuity equation, we can put value of $d\dot{m}$ as

$$d\dot{m} = \rho AV_2 \quad (10)$$

$$d\dot{m} = \rho 2\pi rdrV_2 \quad (11)$$

$$dT = \rho 2\pi rdrV_2\, r^2\omega \quad (12)$$

The angular induction factor accounts for the decrease in torque due to the wake effect. The angular induction factor is given as

$$a' = \frac{\omega}{2\Omega} \quad (13)$$

As $V_2 = V_1\,(1 - a)$, then

$$dT = 4a'(1 - a)\rho V\Omega r^3\pi dr \quad (14)$$

The BEM theory gives us two equations, one is for the axial force and the other for the torque. The power produced at any radius of the rotor is a product of blade angular velocity and torque at that radius as given below

$$dP = \Omega dT \quad (15)$$

The total power is given as

$$P = \int_{rh}^{R} dPdr = \int_{rh}^{R} \Omega dTdr \quad (16)$$

where, r_h is the hub radius. The coefficient of performance (COP) shows the amount of kinetic energy extracted by the wind turbine from the incoming wind and is given as

$$COP = \frac{P}{Pwind} = \frac{\int_{rh}^{R} \Omega dTdr}{\frac{1}{2}\rho\pi R^2 V^3} \quad (17)$$

The coefficient of performance is also given as

$$COP = \frac{8}{\lambda^2}\int_{\lambda_H}^{\lambda} Q{\lambda_r}^2 a'(1-a)\left[1 - \frac{C_D}{C_L}\tan\beta\right] d\lambda_r \quad (18)$$

λ_H is the tip–speed ratio at the hub, λ is the tip–speed ratio, Q takes into account the tip losses, λ_r is the tip–speed ratio at a radius r from the hub, C_L is the coefficient of lift, C_D is the coefficient of drag and β is the relative flow angle onto the blade.

Using Equations (17) and (18), the actual power generated by the wind turbine is given as

$$Power = P = COP\eta\frac{1}{2}\rho\pi R^2 V^3 \quad (19)$$

where η represents the expected electrical and mechanical efficiencies.

3. Methodology

The methodology followed in the current study is summarized in Figure 4. Based on the above-mentioned governing equations, a MATLAB function named "BEM function" was developed, which takes the number of blades, tip–speed ratio, coefficient of lift, stations radii and angle of attack as inputs. These initial input values were selected based on similar studies performed in the literature for designing wind turbines for low-to-medium wind speeds locations [25–27]. The BEM function gives the blade parameters of the selected area in the northern areas of Pakistan. The block diagram of the BEM function is given in Figure 4. The blade parameters are chord-width and angle-of-twist distributions. The number of stations can be increased, which will provide more refined chord-width and angle-of-twist distributions. The chord-width and angle-of-twist distributions are inputs for generating the wind turbine blade profile. After having these parameters, models of turbine were developed in Pro/E. For developing the wind turbine models in Pro/E, the wind turbine blade was divided in various stations. Based on the chord-width and angle-of-twist at each station, the two dimensional cross-sectional profile, as shown in Figure 5a, is sketched at each station. Using the blend option in the Pro/E software, these two-dimensional sketches were combined in the shape of a three-dimensional blade, as shown in Figure 5b. The three-dimensional wind turbine blades and a hub are assembled in Pro/E and were then imported into ADAMS. In order to check the output torque of the wind turbine models, aerodynamic forces were applied on the wind turbine blades.

A MATLAB function named "Aerodynamic function" was developed and used to calculate the wind forces that were applied on Pro/E models in ADAMS environment. The block diagram of the aerodynamic function is given in Figure 4. The aerodynamic function takes the blade parameters as input, and forces at various points on the blade are given at the output. During the first stage, the aerodynamic function carried out an iteration process to find the values of axial and angular induction factors. The axial and angular induction factors are the key terms for finding the energy capture of a specific wind turbine design, working at a specific wind speed. Once the values of axial and angular induction factors are determined, the equations for the forces are used to find the aerodynamic forces. For the Cherat location in the current study, the wind turbine blade was divided into twenty-seven stations. The blade parameters were changed near the hub of wind turbine (in the 9 stations near the hub of the wind turbine), and new models were developed in Pro/E.

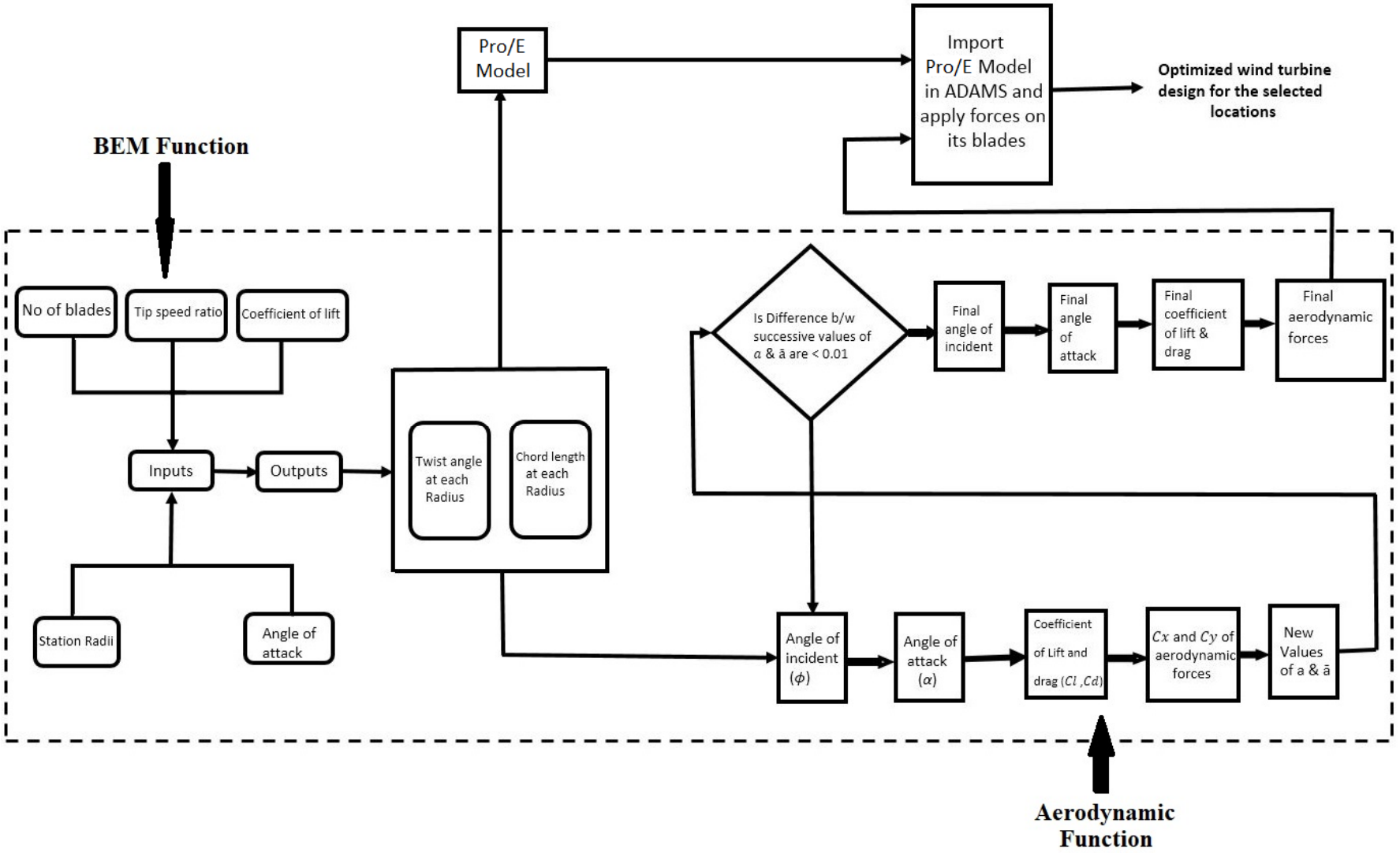

Figure 4. Block diagram of the design process.

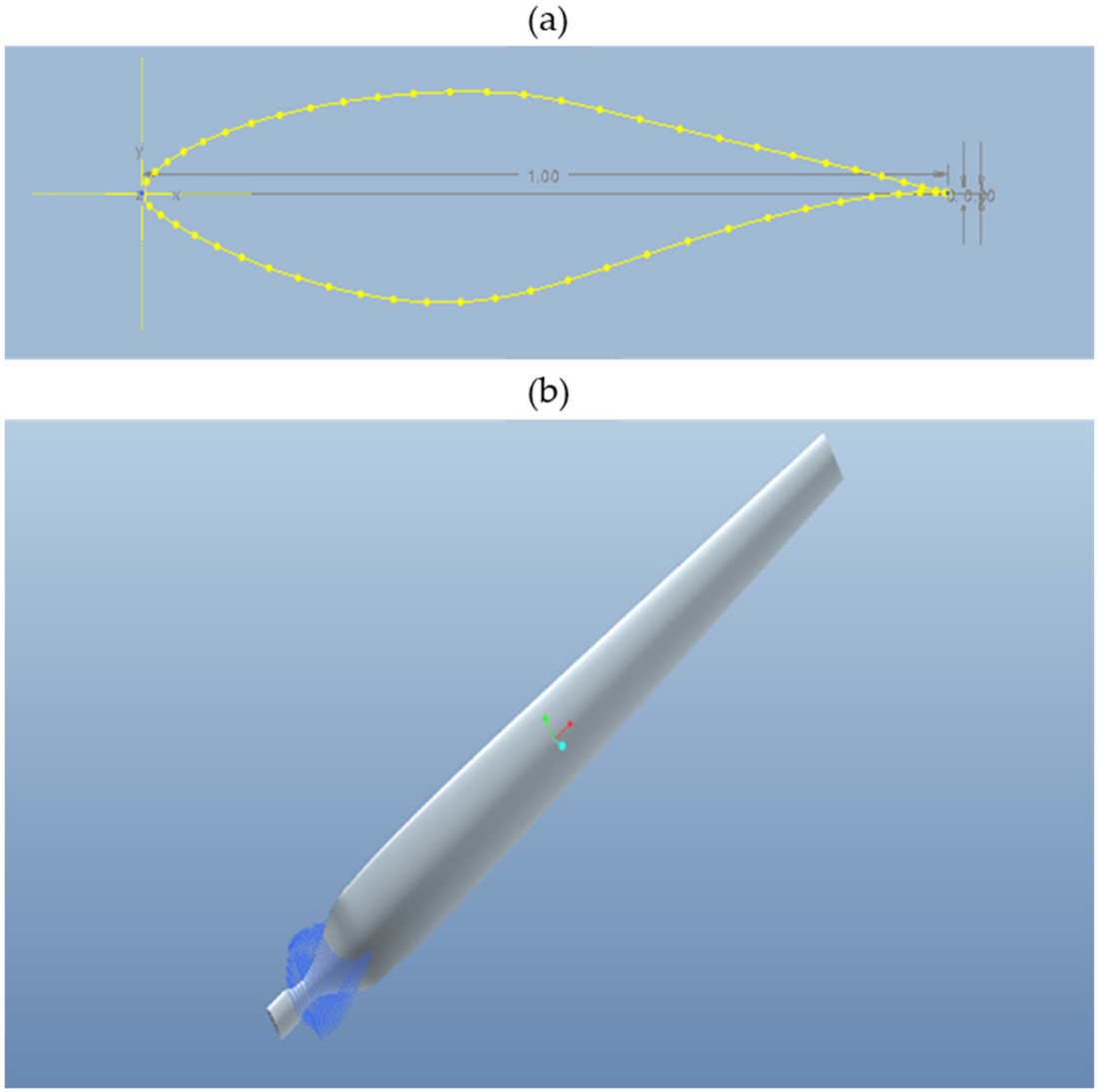

Figure 5. Wind turbine blade modeling in Pro/E software: (**a**) A 2D sketch at a station; (**b**) A 3D blade after combining the 2D sketches at all the stations.

All these models were simulated in ADAMS to find the output torque corresponding to all these models. ADAMS has a full graphical user interface to model the entire mechanical assembly in a single window. The graphical computer-aided design tools in ADAMS can be used to insert a model of a mechanical system in a three-dimensional space or import geometry files such as STEP or IGS. The motion of any two bodies can be constrained in ADAMS by adding a joint between them. A variety of inputs, such as velocities, forces, and initial conditions, can be added to the model in the ADAMS. The behavior of the system can be simulated over time in ADAMS, and it can also animate its motion and compute properties, such as accelerations, forces, torques, etc. ADAMS can be used to analyze extremely complex wind turbine dynamics models. The main advantage of calculating the torque curves using the ADAMS software is that the moment of inertia of the wind turbine is considered during the modeling process. The following steps are used for modeling in ADAMS:

1. Export Pro/E models with IGS format;
2. Import these IGS files into ADAMS;
3. Apply forces on the given models;
4. Carry out simulation settings;
5. Obtain graphs in the ADAMS post-processor.

The various simulation parameters are simulation time, simulation steps, run-time direction of forces, construction of forces, characteristics of forces and magnitude of forces at various points. The number of steps shows the number of points at which the output parameters will be measured in a complete 360-degree rotation of the wind turbine blades. Increasing the number of steps in one complete rotation of wind turbine blades increases the accuracy of output simulations. The run-time direction of force may be space-fixed or body-moving. We have selected the body-moving option for our aerodynamic forces because, at the wind turbine, there is a rotation pattern of wind regarding the wind turbine blades. After assembling the wind turbine model in Pro/E, the model is imported into ADAMS, wind forces are applied on the model at various stations and the various outputs are plotted in the ADAMS post-processor. Finally, the models that had a higher starting torque were selected for the selected location in the northern region of Pakistan.

In Khyber Pakhtoon Khwa (KPK), the Pakistan Meteorological Department (PMD) monitors the wind speed at various locations [32]. Among the various locations, the Cherat location with an average wind speed of 4.2 m/s was selected in the current study. Based on the wind speed monitored by the PMD for the Cherat location, there will be large impacts of seasonal variations on the working of turbines across the year due to the variation in the magnitude of the wind speed. The average wind speed for the Cherat location is 3.56 m/s for the months starting from June until October. This low magnitude of wind speed causes a reduction in the amount of electricity generated by the turbine. The rotor diameter selected in the current study for the selected Cherat location is 5 m.

4. Results and Discussion

Before starting the modelling process of the wind turbine rotor for the selected Cherat location, a validation study was performed. For the validation of the simulation results, the output torque of the simulation is compared with the experimental results. The experimental study was performed for finding the aerodynamics properties of the s809 profile. This model was made from wood. The wood model was exposed to the incident wind of various speeds. The speed of the incident wind was measured by an anemometer and the rpm of the wind turbine shaft was measured by a digital tachometer. For a certain wind speed, the torque at the wind turbine shaft was calculated by a spring balance arrangement. A spring balance was attached to the shaft of the wind turbine at both sides. The tension difference on both sides when multiplied by the radius of the shaft gives the output torque. The values of the torque were calculated at various wind speeds. As the wind turbine was exposed to the cross wind, it was expected that there would be a slight difference between the experimental and simulation results. A similar model was developed in Pro/E and simulated in ADAMS. A three-blade wind turbine model was assembled with hub in Pro/E assembly mode. This model is shown in Figure 6. This model was then imported to ADAMS. For various wind speeds, aerodynamic forces were calculated using MATLAB function. These forces were applied to the wind turbine model in the ADAMS environment.

The output torque for various wind speeds is shown in Figure 7. It can be seen in Figure 7 that during the starting phase, the value of the torque is very low, and normally, it is not enough to overcome the static friction of the wind turbine. The starting torque is critical for the self-starting of the wind turbine at low-to-medium wind speeds.

The torque output from the simulation was compared with the experimental results after 10 s. The comparison shows that the simulation results are in good agreement with the experimental results. Although there is a specific difference between the output values of torque from simulation and experiment, the difference is within a small range, which is due to the above-mentioned reason of the cross flow of the wind and the number of stations that are selected during the wind turbine blade profile development. The difference can be decreased by increasing the number of stations in the Pro/E model. The actual number of stations can be selected once the experimental values are obtained. The comparison is shown Table 1.

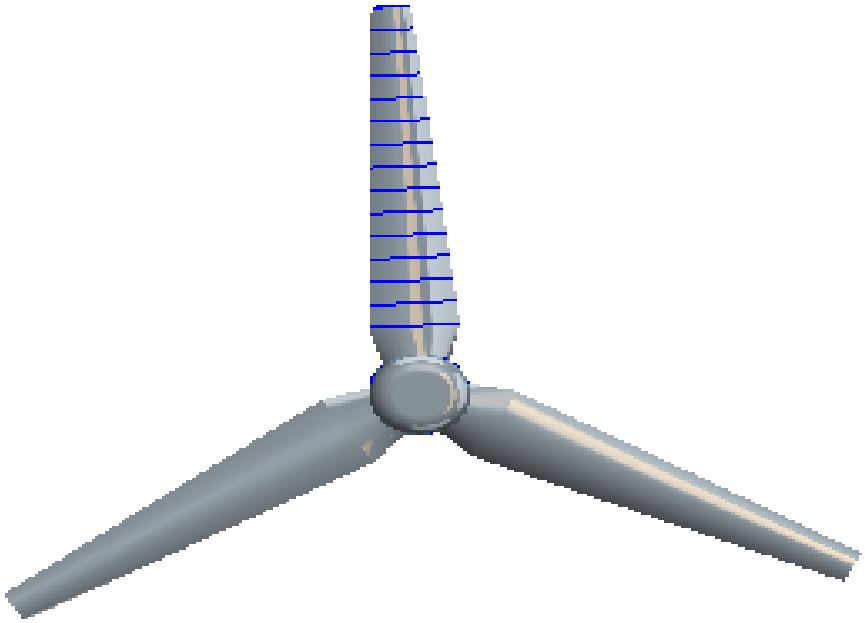

Figure 6. Assembled model for experimental wind turbine design.

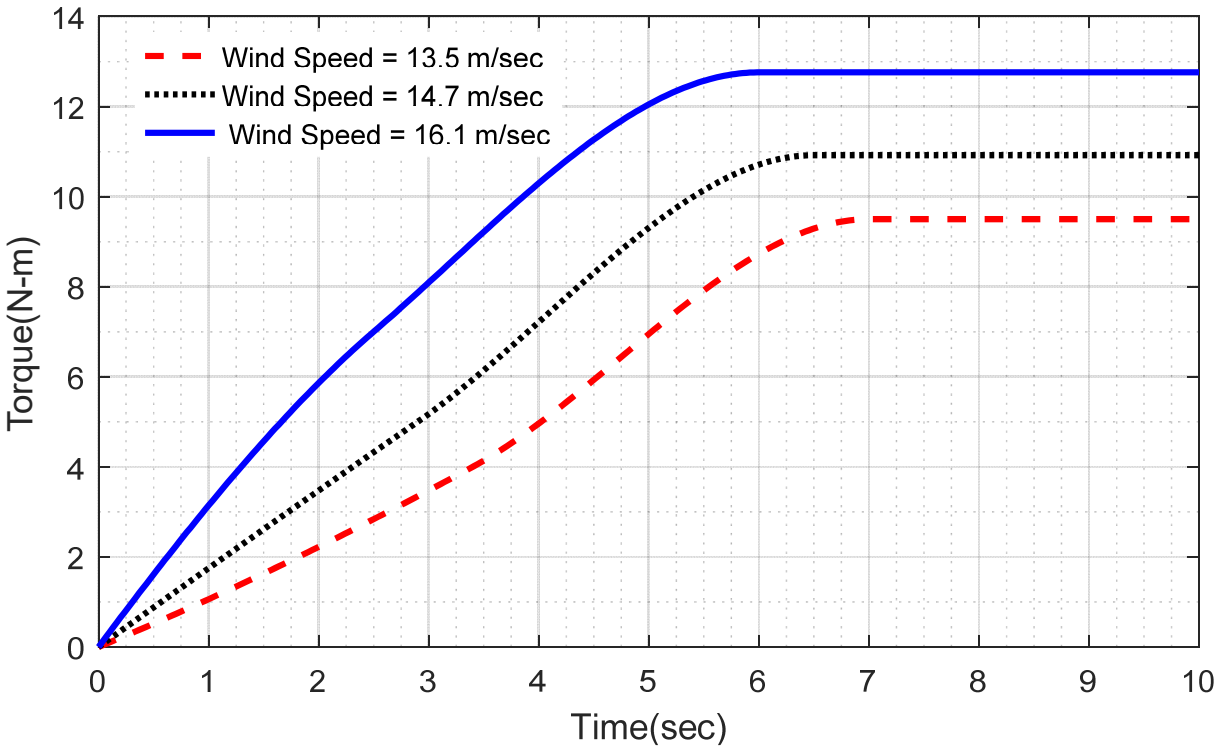

Figure 7. Output torque for various wind speeds.

Table 1. Comparison of the simulation and experimental results.

Wind Speed (m/s)	Torque from Simulation (N-m)	Torque from Experiment (N-m)
13.50	9.50	9.10
14.70	10.92	10.20
16.10	12.76	12.90

After model validation, the initial Pro/E model similar to Figure 6 was constructed for the Cherat region and was imported to ADAMS for the calculation of torque. The torque output is shown in Figure 8a. Next, the chord lengths of the wind turbine blades are increased near the hub of the wind turbine (in the nine stations near the hub of the wind turbine). The torque output is shown in Figure 8b. If the magnitude of the torque is compared in Figure 8a,b after 5 s, it can be observed that the starting torque is increased by increasing the chord lengths.

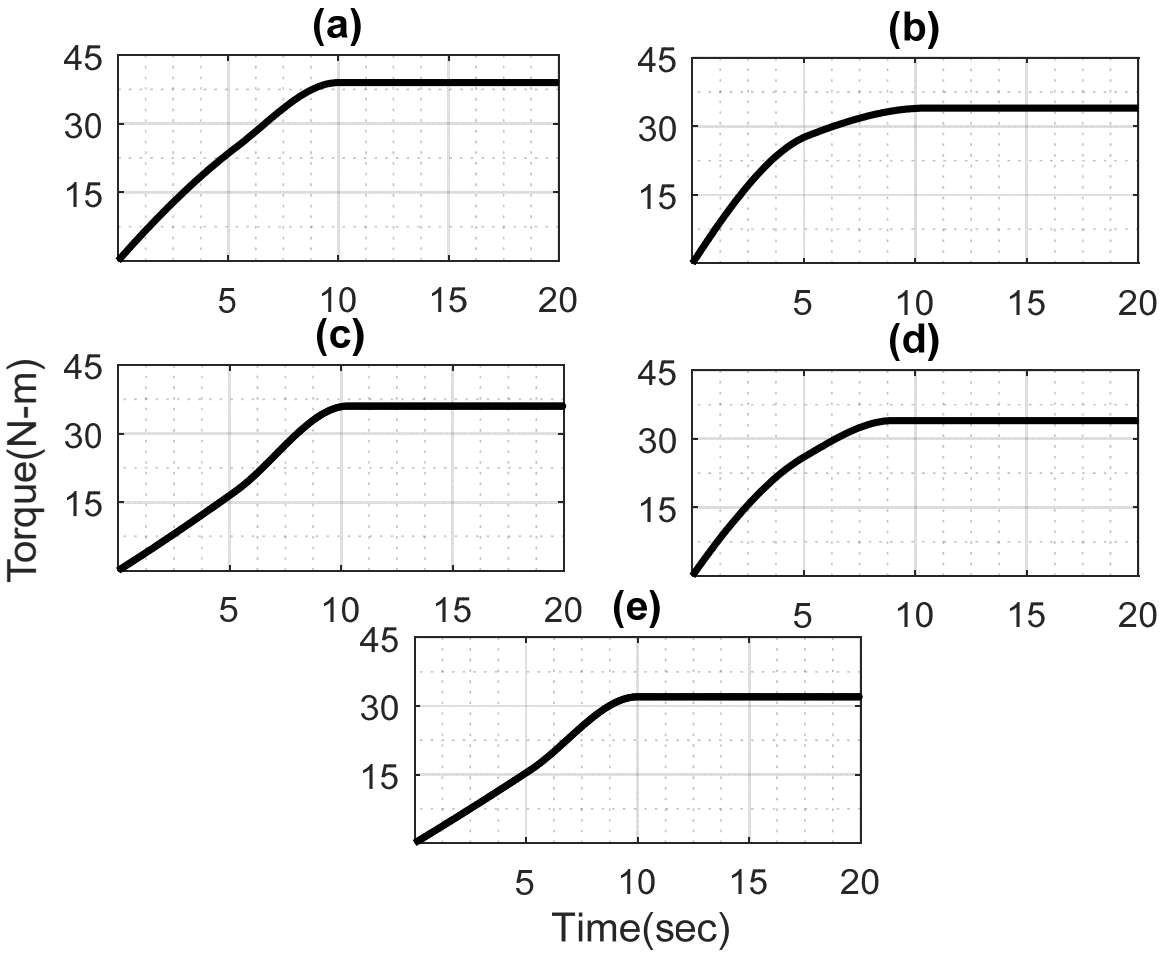

Figure 8. The output torque for the Cherat location: (**a**) For the initial model; (**b**) For the increasing chord lengths model; (**c**) For the decreasing chord lengths model; (**d**) For the increasing blade angles model; (**e**) For the decreasing blade angles model.

Next, the chord lengths of the wind turbine blades are decreased near the hub of the wind turbine (in the nine stations near the hub of the wind turbine). The torque output is shown in Figure 8c. If the magnitude of the torque is compared in Figure 8a,c after 5 s, it can be observed that the starting torque is decreased by decreasing the chord lengths.

In the next case, the blade angles of the wind turbine blades are increased near the hub of the wind turbine (in the nine stations near the hub of the wind turbine). The torque output is shown in Figure 8d. If the magnitude of the torque is compared in Figure 8a,d after 5 s, it can be observed that the starting torque is increased by increasing the blade angles.

In the last case, the blade angles of the wind turbine blades are decreased near the hub of the wind turbine (in the nine stations near the hub of the wind turbine). The torque output is shown in Figure 8e. If the magnitude of the torque is compared in Figure 8a,e after 5 s, it can be observed that the starting torque is decreased by decreasing the blade angles.

The methodology followed in the current study for increasing the initial torque by the alteration of the part of the wind turbine blades near the hub is a very efficient and

easily implemented strategy compared to other strategies based on changing the number of blades or using various mechanisms for blade pitching. In Figure 8, it is also confirmed that the starting of the wind turbine is mainly dependent on the blade profile near the hub region because the alteration of the blade parameters near the hub of the wind turbine has caused excessive variations in the magnitude of the starting torque.

The COP of the above-mentioned cases is shown in Figure 9. The COP shows the amount of kinetic energy extracted by wind turbine from the incoming wind. Based on Equations (17) and (18), the COP of the wind turbine is dependent on the tip–speed ratio, tip losses, the coefficient of lift, the coefficient of drag and the relative flow angle onto the blade. The COP is a very important factor during the wind turbine design because, based on Equation (19), the actual power generated by the wind turbine is mainly dependent on the value of the COP for the wind turbine.

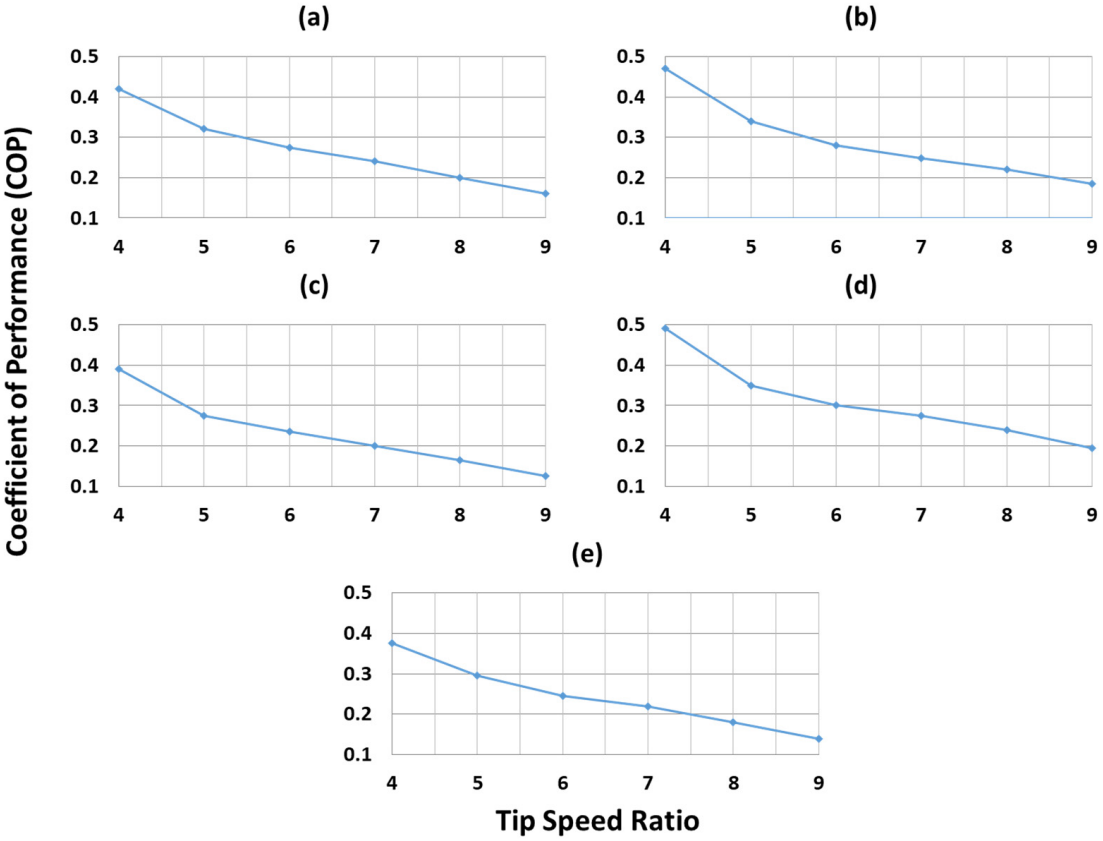

Figure 9. COP of the various designs for the Cherat location: (**a**) For the initial model; (**b**) For the increasing chord lengths model; (**c**) For the decreasing chord lengths model; (**d**) For the increasing blade angles model; (**e**) For the decreasing blade angles model.

It can be seen from Figure 9 that the COP of the wind turbine decreases by decreasing the chord width and blade angles near the hub of the wind turbine (in the nine stations near the hub of the wind turbine). The COP increases by increasing the chord length and blade angles near the hub of the wind turbine (in the nine stations near the hub of the wind turbine).

The distribution of the chord widths and blade angles for the above-mentioned cases is given in Table 2. There are five designs given in Table 2 for the Cherat location. Each design consists of the values of the chord-width and blade angles at twenty-seven stations of the wind turbine blades. Each column in Table 2 corresponds to a station on the wind turbine blade. Based on Figures 8 and 9, the blade parameters corresponding to the increasing chord widths and blade angles will give a maximum starting torque and COP.

Table 2. Chord width and blade angle distributions at various stations of the wind turbine blades for the various cases.

Initial Model	Chord Width	0.710	0.658	0.613	0.574	0.539	0.508	0.480	0.455	0.433	0.413	0.394	0.377	0.361	0.347	0.334	0.321	0.310	0.299	0.289	0.280	0.271	0.263	0.255	0.248	0.241	0.235	0.228
	Blade Angles	0.394	0.327	0.275	0.233	0.110	0.172	0.148	0.128	0.111	0.096	0.083	0.072	0.061	0.052	0.044	0.036	0.029	0.023	0.017	0.012	0.007	0.003	−0.001	−0.005	−0.009	−0.012	−0.015
Increasing Chord Width Model	Chord Width	0.981	0.910	0.847	0.792	0.744	0.702	0.663	0.629	0.598	0.413	0.394	0.377	0.361	0.347	0.334	0.321	0.310	0.299	0.289	0.280	0.271	0.263	0.255	0.248	0.241	0.235	0.228
	Blade Angles	0.394	0.327	0.275	0.233	0.110	0.172	0.148	0.128	0.111	0.096	0.083	0.072	0.061	0.052	0.044	0.036	0.029	0.023	0.017	0.012	0.007	0.003	−0.001	−0.005	−0.009	−0.012	−0.015
Decreasing Chord Width Model	Chord Width	0.679	0.630	0.587	0.549	0.520	0.486	0.460	0.440	0.414	0.413	0.394	0.377	0.361	0.347	0.334	0.321	0.310	0.299	0.289	0.280	0.271	0.263	0.255	0.248	0.241	0.235	0.228
	Blade Angles	0.394	0.327	0.275	0.233	0.110	0.172	0.148	0.128	0.111	0.096	0.083	0.072	0.061	0.052	0.044	0.036	0.029	0.023	0.017	0.012	0.007	0.003	−0.001	−0.005	−0.009	−0.012	−0.015
Increasing Blade Angle Model	Chord Width	0.710	0.658	0.613	0.574	0.539	0.508	0.480	0.455	0.433	0.413	0.394	0.377	0.361	0.347	0.334	0.321	0.310	0.299	0.289	0.280	0.271	0.263	0.255	0.248	0.241	0.235	0.228
	Blade Angles	0.446	0.380	0.327	0.286	0.252	0.224	0.201	0.181	0.164	0.096	0.083	0.072	0.061	0.052	0.044	0.036	0.029	0.023	0.017	0.012	0.007	0.003	−0.001	−0.005	−0.009	−0.012	−0.015
Decreasing Blade Angle Model	Chord Width	0.710	0.658	0.613	0.574	0.539	0.508	0.480	0.455	0.433	0.413	0.394	0.377	0.361	0.347	0.334	0.321	0.310	0.299	0.289	0.280	0.271	0.263	0.255	0.248	0.241	0.235	0.228
	Blade Angles	0.341	0.275	0.222	0.181	0.147	0.119	0.096	0.076	0.059	0.096	0.083	0.072	0.061	0.052	0.044	0.036	0.029	0.023	0.017	0.012	0.007	0.003	−0.001	−0.005	−0.009	−0.012	−0.015

5. Conclusions

Optimized wind turbine design was obtained for the Cherat location of Pakistan. Three-bladed wind turbine models were simulated in the ADAMS environment. Starting is not usually the primary concern of the designer; however, a simple method of predicting a turbine's starting performance is useful, particularly if the sitting turbines are in low or unsteady winds. The method described here is suitable for this purpose.

- The BEM theory was used to calculate the initial wind turbine blade parameters. Different blade profiles were developed from the initial wind turbine blade profile by varying the chord lengths and blade angles. Increasing the cord lengths and blade angles near the hub region increases the output starting torque. If the magnitude of the starting torque is compared after 5 s for the various cases simulated in the current study, it can be concluded that increasing the blade angles and chord-width near the hub of the wind turbine will increase the magnitude of the starting torque. As compared to the initial wind turbine model, for the optimized wind turbine model, the starting torque (measured after 5 s) increased, from 22.5 N-m to 28 N-m;
- The slope of the torque curve increases with an increase in the values of the blade angles and the chord-width near the hub of the wind turbine. With this rapid increase in the magnitude of the torque during the initial period, the starting behavior of the wind turbine will be improved;
- Decreasing the cord lengths and blade angles near the hub region decreases the output starting torque. If the magnitude of the starting torque is compared after 5 s for the various cases simulated in the current study, it can be concluded that decreasing the blade angles and chord-width near the hub of the wind turbine will decrease the magnitude of the starting torque;
- The COP increases by increasing the chord length and blade angles at various stations of the wind turbine blades. The blade parameters corresponding to the increasing chord widths and blade angles will give a maximum starting torque and COP. COP increased from 0.42 to 0.49 at a tip–speed ratio of 4 for the optimized wind turbine model.

Funding: This research received no external funding.

Institutional Review Board Statement: Not applicable.

Informed Consent Statement: Not applicable.

Data Availability Statement: The data are available by contacting the corresponding author.

Acknowledgments: The author appreciates and acknowledges the support provided by the King Fahd University of Petroleum and Minerals (KFUPM) by providing all the essential resources to conduct this study.

Conflicts of Interest: The author declares no conflict of interest.

References

1. Liu, D.; Guo, X.; Xiao, B. What causes growth of global greenhouse gas emissions? Evidence from 40 countries. *Sci. Total Environ.* **2019**, *661*, 750–766. [CrossRef] [PubMed]
2. Usman, M.; Helal, A.; Abdelnaby, M.M.; Alloush, A.M.; Zeama, M.; Yamani, Z.H. Trends and prospects in UiO-66 metal-organic framework for CO_2 capture, separation, and conversion. *Chem. Rec.* **2021**, *21*, 1771–1791. [CrossRef] [PubMed]
3. Khan, S.; Khulief, Y.A.; Al-Shuhail, A. Mitigating climate change via CO_2 sequestration into Biyadh reservoir: Geomechanical modeling and caprock integrity. *Mitig. Adapt. Strateg. Glob. Chang.* **2019**, *24*, 23–52. [CrossRef]
4. Rehman, S.; Alam, M.M.; Alhems, L.M.; Rafique, M.M. Horizontal axis wind turbine blade design methodologies for efficiency enhancement—A review. *Energies* **2018**, *11*, 506. [CrossRef]
5. Alam, M.; Chowdhury, T.A.; Dhar, A.; Al-Ismail, F.S.; Choudhury, M.S.H.; Shafiullah, M.; Hossain, M.; Ullah, A.; Rahman, S.M. Solar and wind energy integrated system frequency control: A critical review on recent developments. *Energies* **2023**, *16*, 812. [CrossRef]
6. Melikoglu, M. Geothermal energy in Turkey and around the World: A review of the literature and an analysis based on Turkey's Vision 2023 energy targets. *Renew. Sustain. Energy Rev.* **2017**, *76*, 485–492. [CrossRef]

7. Tefera, W.M.; Kasiviswanathan, K.S. A global-scale hydropower potential assessment and feasibility evaluations. *Water Resour. Econ.* **2022**, *38*, 100198. [CrossRef]
8. Tabriz, Z.H.; Khani, L.; Mohammadpourfard, M.; Akkurt, G.G. Biomass driven polygeneration systems: A review of recent progress and future prospects. *Process Saf. Environ. Prot.* **2023**, *169*, 363–397. [CrossRef]
9. Herbert, G.J.; Iniyan, S.; Sreevalsan, E.; Rajapandian, S. A review of wind energy technologies. *Renew. Sustain. Energy Rev.* **2007**, *11*, 1117–1145. [CrossRef]
10. Maradin, D. Advantages and disadvantages of renewable energy sources utilization. *Int. J. Energy Econ. Policy* **2021**, *11*, 176–183. [CrossRef]
11. Adnan, A.; Khan, S. Designing and modeling of airborne wind energy system. In Proceedings of the 13th International Conference on Mechanical and Aerospace Engineering (ICMAE), Bratislava, Slovakia, 20–22 July 2022.
12. Adnan, A.; Khan, S. A comparative study of various strategies used for the mitigation of global warming. In Proceedings of the Thriving Through Climate Change & Pandemic Conference, Windsor, ON, Canada, 24–25 June 2021.
13. Wind Electricity. Available online: https://www.iea.org/reports/wind-electricity (accessed on 10 January 2023).
14. Cheng, K.; Wang, Z.; He, Y.; Yang, G. The comparison of theoretical potential application of two types of wind turbines in Northern Shaanxi. In Proceedings of the Asia-Pacific Power and Energy Engineering Conference, Shanghai, China, 27–29 March 2012. [CrossRef]
15. Chawla, J.S.; Suryanarayanan, S.; Puranik, B.; Sheridan, J.; Falzon, B.G. Efficiency improvement study for small wind turbines through flow control. *Sustain. Energy Technol. Assess.* **2014**, *7*, 195–208. [CrossRef]
16. Bensalah, A.; Barakat, G.; Amara, Y. Electrical generators for large wind turbine: Trends and challenges. *Energies* **2022**, *15*, 6700. [CrossRef]
17. Morcos, V.H. Aerodynamic performance analysis of horizontal axis wind turbines. *Renew. Energy* **1994**, *4*, 505–518. [CrossRef]
18. Yang, J.; Fang, L.; Song, D.; Su, M.; Yang, X.; Huang, L.; Joo, Y.H. Review of control strategy of large horizontal-axis wind turbines yaw system. *Wind Energy* **2021**, *24*, 97–115. [CrossRef]
19. Tang, X.; Huang, X.; Peng, R.; Liu, X. A direct approach of design optimization for small horizontal axis wind turbine blades. *Procedia CIRP* **2015**, *36*, 12–16. [CrossRef]
20. *IEC 61400–2*; Wind Turbines—Part 2: Small Wind Turbines. International Electrotechnical Commission: London, UK, 2013; ISBN 978-2-8322-1284-4.
21. Kelele, H.K.; Frøyd, L.; Kahsay, M.B.; Nielsen, T.K. Characterization of aerodynamics of small wind turbine blade for enhanced performance and low cost of energy. *Energies* **2022**, *15*, 8111. [CrossRef]
22. Gitano-Briggs, H. Low speed wind turbine design. In *Advances in Wind Power*; IntechOpen: London, UK, 2012; ISBN 978-953-51-0863-4.
23. Chu, Y.J.; Lam, H.F.; Peng, H.Y. Numerical investigation of the power and self-start performance of a folding-blade horizontal axis wind turbine with a downwind configuration. *Int. J. Green Energy* **2022**, *19*, 28–51. [CrossRef]
24. Mitchell, S.; Ogbonna, I.; Konstantin, V. Improvement of self-starting capabilities of vertical axis wind turbines with new design of turbine blades. *Sustainability* **2021**, *13*, 3854. [CrossRef]
25. Akour, S.N.; Al-Heymari, M.; Ahmed, T.; Khalil, K.A. Experimental and theoretical investigation of micro wind turbine for low wind speed regions. *Renew. Energy* **2018**, *116*, 215–223. [CrossRef]
26. Wright, A.K.; Wood, D.H. The starting and low wind speed behavior of a small horizontal axis wind turbine. *J. Wind. Eng. Ind. Aerodyn.* **2000**, *92*, 1265–1279. [CrossRef]
27. Ebert, P.R.; Wood, D.H. Observations of the starting behavior of a small horizontal axis wind turbine. *Renew. Energy* **1997**, *12*, 245–257. [CrossRef]
28. Supakit, W.; Grant, L.I.; Robert, G.D. The physics of H-Darrieus turbine starting behavior. *J. Eng. Gas Turbines Power* **2016**, *138*, 1–11.
29. Sun, X.; Zhu, J.; Li, Z.; Sun, G. Rotation improvement of vertical axis wind turbine by offsetting pitching angles and changing blade numbers. *Energy* **2021**, *215*, 119177. [CrossRef]
30. Mohamed, O.S.; Elbaz, A.M.; Bianchini, A. A better insight on physics involved in the self-starting of a straight-blade Darrieus wind turbine by means of two-dimensional Computational Fluid Dynamics. *J. Wind. Eng. Ind. Aerodyn.* **2021**, *218*, 104793. [CrossRef]
31. Wind Turbine Blade Analysis Using the Blade Element Momentum Method. Available online: https://community.dur.ac.uk/g.l.ingram/download/wind_turbine_design.pdf (accessed on 10 January 2023).
32. Pakistan Meteorological Department, Wind Energy Project. Available online: http://www.pmd.gov.pk/wind/wind_project_files/Page351.html (accessed on 10 January 2023).